

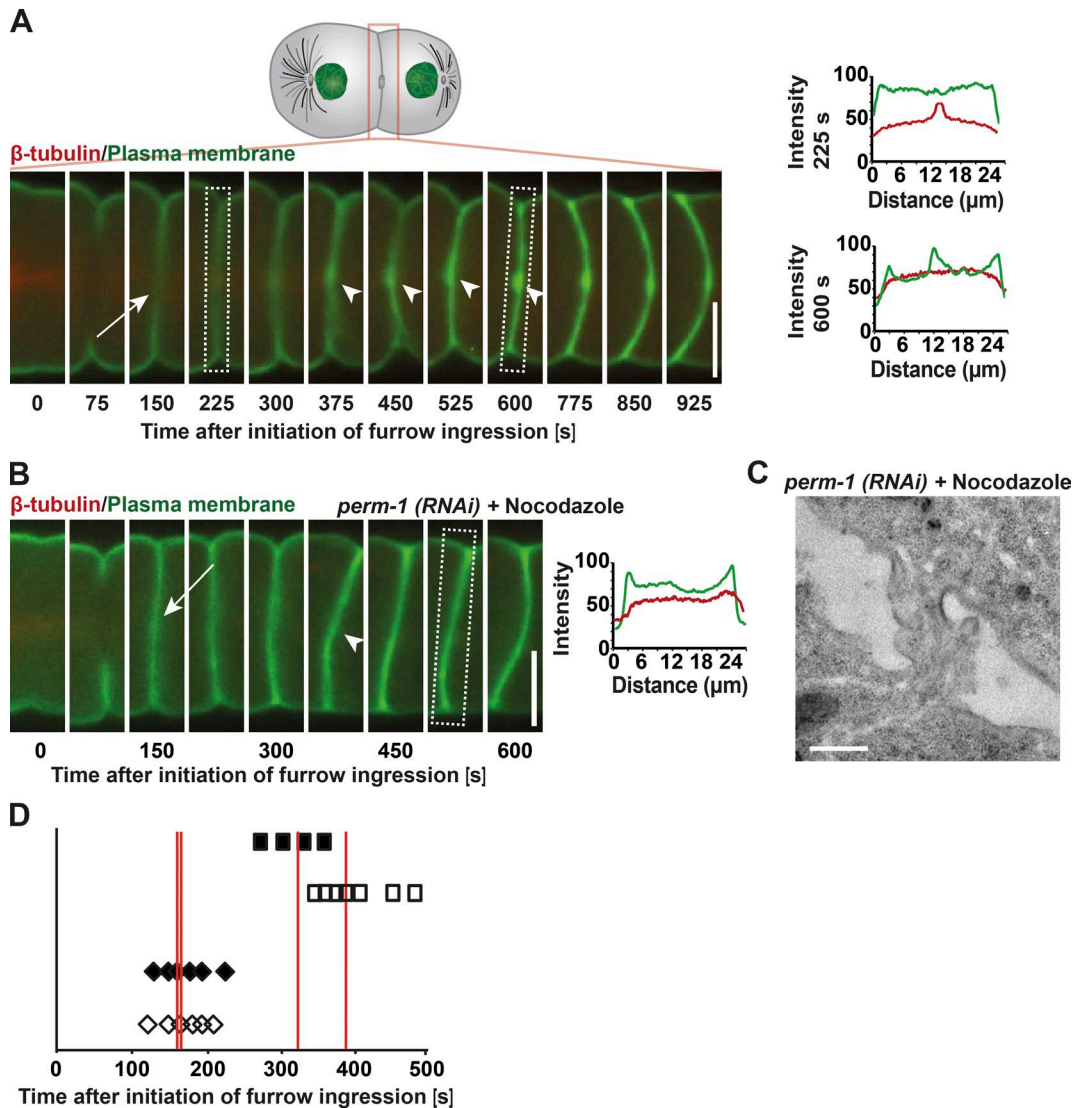
König et al., <https://doi.org/10.1083/jcb.201607030>

Figure S1. **Membrane accumulation during furrow ingression.** (A) Spinning-disk confocal optics were used to image a dividing *C. elegans* embryo coexpressing mCherry:: β -tubulin and GFP::PH. The time points of cleavage furrow closure (arrow) and membrane accumulation at the midbody (arrowheads) are highlighted. Line scan analysis within the boxed regions was used to measure the fluorescence intensities of the GFP::PH probe relative to tubulin at 225 and 600 s (right). $n = 10$. (B) Embryos from a *perm-1(RNAi)*-treated transgenic animal coexpressing mCherry:: β -tubulin and GFP::PH were imaged after treatment with nocodazole (added upon onset of cleavage furrow ingression). The time point of cleavage furrow closure (arrow) and the lack of membrane accumulation (arrowhead) are highlighted. Line scan analysis within the boxed region was used to measure the fluorescence intensities of the GFP::PH probe relative to tubulin (right). $n = 10$. (C) The intercellular bridge of a nocodazole-treated embryo was imaged using electron microscopy ~ 240 s after onset of furrow ingression. Microtubules are not detectable within the intercellular bridge. Bars: (A and B) 10 μm ; (C) 500 nm. (D) Timing of events in control and *perm-1(RNAi)*-treated embryos. Cleavage furrow closure (open diamonds, control; closed diamonds, PERM-1-depleted embryos) and microtubule disassembly (open squares, control; closed squares, PERM-1-depleted embryos) are shown. Red lines highlight the mean time point of cleavage furrow closure and microtubule disassembly. $n = 10$.

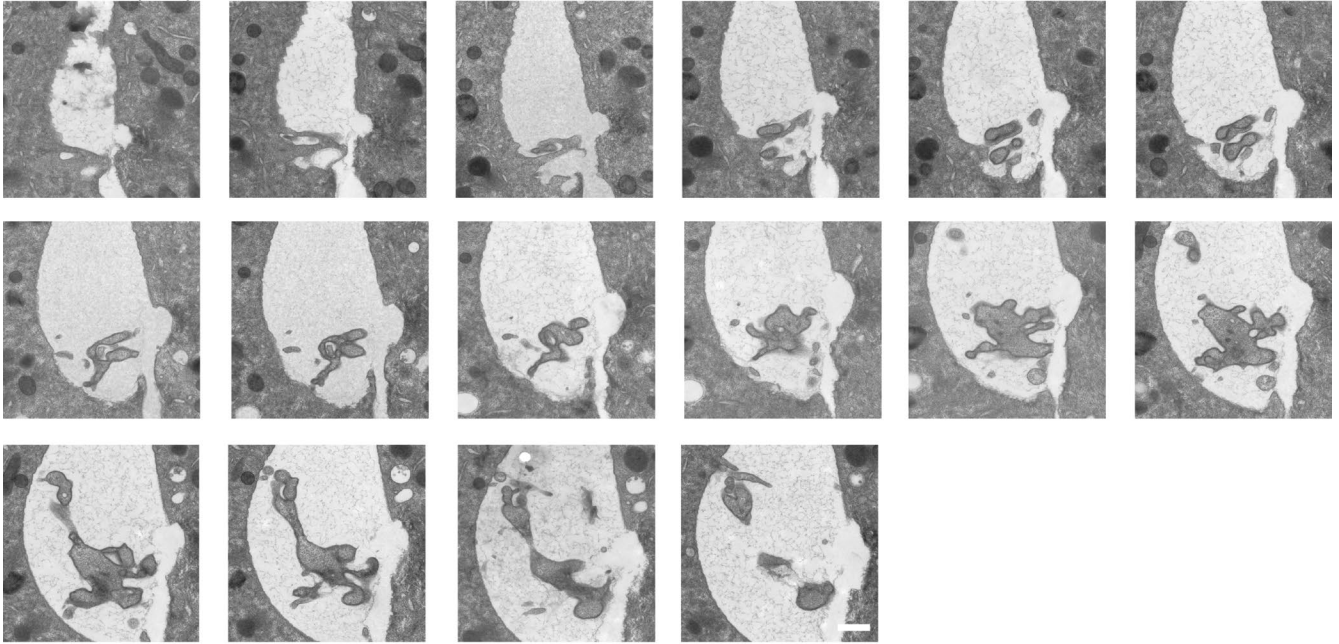
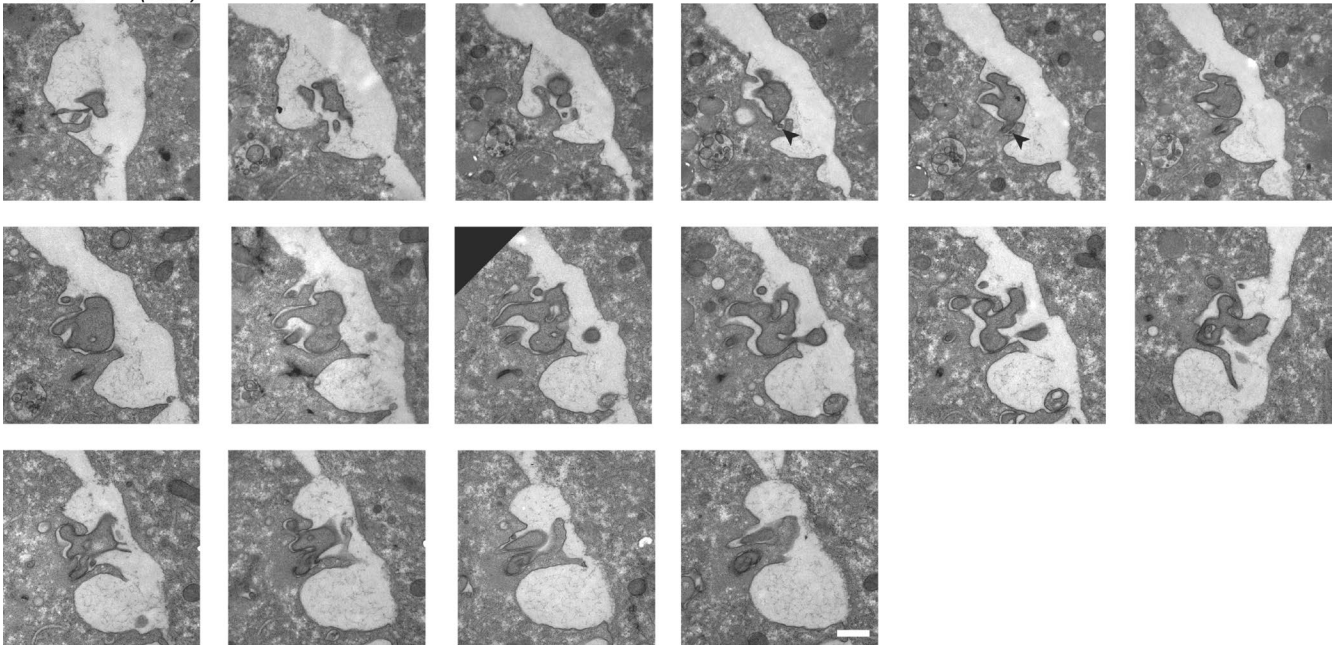
A**ESCRT-I^{tsg-101} (RNAi)****B****ESCRT-I^{tsg-101} (RNAi)**

Figure S2. **ESCRT function is dispensable for the first membrane scission event during cytokinesis in *C. elegans*.** (A and B) Serial thin-section electron micrographs of two different *tsg-101*(RNAi) embryos undergoing abscission ~1,100 s after initiation of furrow ingression. The connection of the intercellular bridge to one of the daughter cells is indicated (arrowheads). Bars, 500 nm.

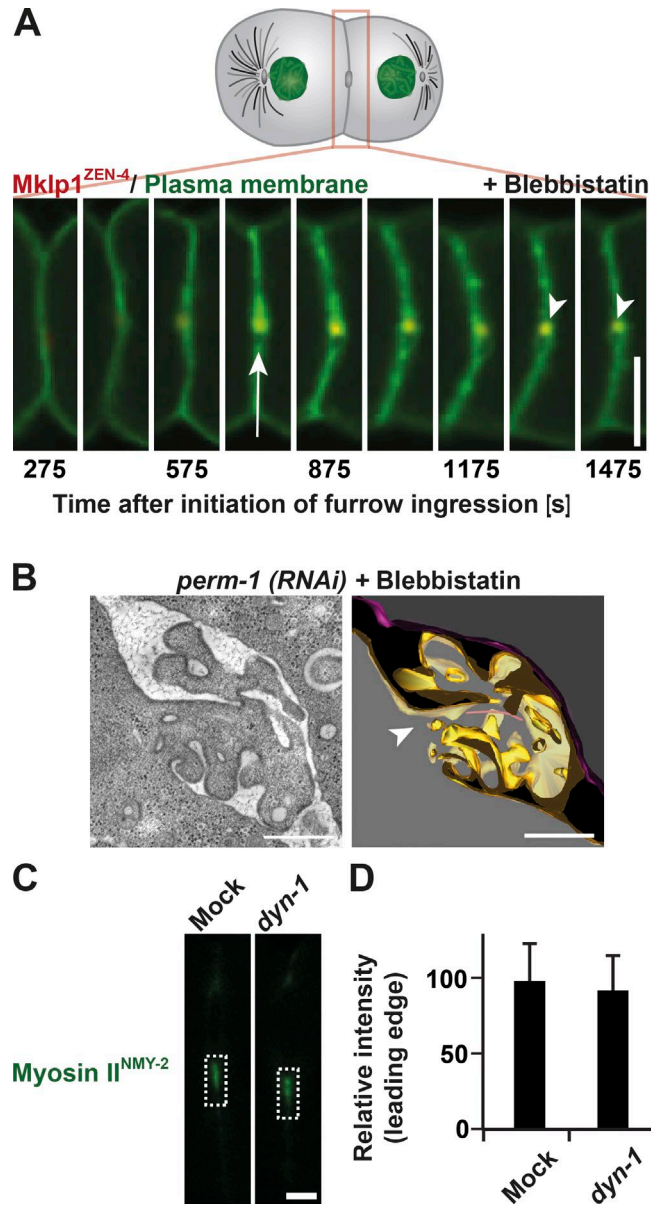
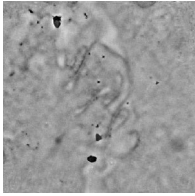
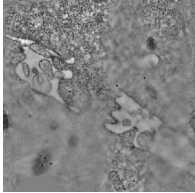


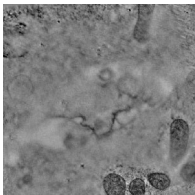
Figure S3. **Myosin II function is required for cytokinetic abscission.** (A) Representative still images of a Blebbistatin-treated embryo during the late stages of cytokinesis. The drug was added after the completion of furrow ingression. Localization of the midbody marker MKLP1^{ZEN-4} is indicated (arrow). Engulfment of the midbody remnant into the posterior cell failed (arrowheads). Bar, 10 μ m. $n = 10$. (B) Tomographic slice (left) and 3D model (right) of a high-pressure frozen Blebbistatin-treated embryo. An arrowhead indicates the connection of the AB cell to the intercellular bridge. The membrane of the intercellular bridge is highlighted in gold. Bar, 500 nm. (C) Myosin II distribution on the ingressing furrow is not affected by DYN-1 depletion. Representative still images of control and *dyn-1(RNAi)* embryos taken \sim 100 s after initiation of furrow ingression. The regions used for fluorescence intensity measurements are highlighted (boxed areas). Bar, 2 μ m. $n = 6$ embryos for each condition. (D) Relative fluorescence intensity of myosin II at the leading edge of the cleavage furrow in mock-treated and DYN-1-depleted embryos compared with control embryos. Error bars show SD. $n = 6$ for each condition.



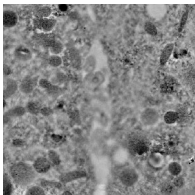
Video 1. **Tomographic reconstruction and 3D modeling of the first intercellular bridge in the early *C. elegans* embryo.** The time point of freezing after initiation of furrow ingression is 240 s. The video corresponds to Fig. 1 C. This video was shot at 10 frames per second.



Video 2. **Tomographic reconstruction and 3D modeling of the first intercellular bridge in the early *C. elegans* embryo.** The time point of freezing after initiation of furrow ingression is 375 s. The video corresponds to Fig. 1 C. This video was shot at 10 frames per second.



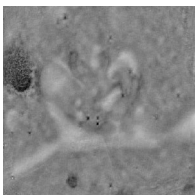
Video 3. **Tomographic reconstruction and 3D modeling of the first intercellular bridge in the early *C. elegans* embryo.** The time point of freezing after initiation of furrow ingression is 445 s. The video corresponds to Fig. 1 C. This video was shot at 10 frames per second.



Video 4. **Tomographic reconstruction and 3D modeling of the first intercellular bridge in the early *C. elegans* embryo.** The time point of freezing after initiation of furrow ingression is 650 s. The video corresponds to Fig. 1 C. This video was shot at 10 frames per second.



Video 5. **Tomographic reconstruction and 3D modeling of the first intercellular bridge in the early *C. elegans* embryo.** The time point of freezing after initiation of furrow ingression is 765 s. The video corresponds to Fig. 1 C. This video was shot at 10 frames per second.



Video 6. **Tomographic reconstruction and 3D modeling of the first intercellular bridge in the early *C. elegans* embryo.** The time point of freezing after initiation of furrow ingression is 900 s. The video corresponds to Fig. 1 C. This video was shot at 10 frames per second.